Supporting Information

Boareto et al. 10.1073/pnas.1416287112

SI Text

S1. Parameters' Values and Assumptions

Our model is based on the model proposed by Sprinzak et al. (1), which well-fitted their experimental results designed to measure the interaction between Notch and Delta, both in *cis*- and *trans*-. Their experimental results suggest a Hill coefficient for Notch activity close to 2 and this value was chosen to represent the NICD activation of Notch (n_N) and inhibition of Delta (n_D). For the case of NICD modulation of Jagged, a higher Hill coefficient ($n_J = 5$) was chosen to represent both direct activation of Jagged by NICD and indirect modulations by miRNA—Jagged is strongly repressed by miR200 (2); however, miR200 is repressed by Snail (3), which in turn is activated by NICD (4), resulting in a effective strong activation of Jagged by the signal. A strong activation of Jagged is required for the maintenance of the (S/R). As shown in Fig. S6, for $n_J = 4$ the range of existence of the S/R state is significantly decreased and for $n_J = 3$ this state is no longer observed. Previous work (1) shows that *cis*-inhibition rate (k_C) is approximately 10 times higher than transactivation rate (k_T) for Notch–Delta interaction and we assumed the same values for Notch–Jagged interaction when the effect of Fringe is not taken into account. Unlike the previous model (1) in which the rates are in units of relative fluorescence units, our variables represent the number of proteins in the membrane for Notch, Delta, and Jagged, and the number of proteins inside the nucleus for the signal (NICD). Because of that, we scaled the values of *cis*-inhibition and *trans*-activation rate accordingly.

The rapid degradation of the signal is an important feature in the Notch signaling (5) and, because of that, we considered the NICD degradation rate (γ_I) to be 5 times higher than the typical protein degradation rate $\gamma = 0.1\ \mathrm{h}^{-1}$. The values of N_0, D_0, and J_0 which represent the production rate of the proteins were chosen to keep the maximum number of proteins in the membrane up to ~5,000 per cell. This value is consistent with experimental results where the concentration of the proteins varies up to a few hundred ng/ml (6)—or a few thousand proteins per cell. Once most proteins are exported to the membrane, we should expect a few thousand proteins in the membrane when the expression is up-regulated. Similarly, the number of NICD inside the nucleus varies up to a few hundreds and because of that, we select the threshold of the Hill function (I_0) to be 200.

For the effect of glycosylation of Notch by Fringe, we assumed that the fraction of glycosylated Notch increases with the signal (NICD), represented by a Hill coefficient ($n_F = 1$). We assumed that glycosylation of Notch increases its affinity to Delta by a factor of 3 ($\lambda_D^F = 3.0$) and decrease its affinity to Jagged by 70% ($\lambda_J^F = 0.3$). Experimental evidence for modulation of Notch by lunatic Fringe shows a 4.4-fold reduction for Jagged1-mediated signaling and at least a twofold increase for Delta1-mediated signaling (7). Finally, $\lambda_N = \lambda_J = 2.0$ for Notch and Jagged represents an activation of their production by the signal and $\lambda_D = 0.0$ for Delta represents its inhibition by the signal.

Assumptions of the Model.

i) Degradation rates of Notch, Delta, and Jagged are the same.
ii) Number of receptor and ligands are on the order of thousands of molecules when overexpressed and the number of NICD inside the nucleus is on the order of hundreds of molecules.
iii) The affinity between Notch–Delta and Notch–Jagged is the same when Notch is not modified by Fringe.
iv) Jagged is strongly activated by NICD due to both direct and indirect activation; therefore, we assumed a high Hill coefficient for this activation ($n_J = 5$).
v) Fringe is activated by NICD and we assumed that the number of Notch modified by Fringe increases with the levels of NICD. We did not consider the delay in this modification that might occur due to the production of Fringe.

S2. Model Details

To include the effect of glycosylation of Notch by Fringe we considered two types of Notch, whether it is modified or not by Fringe. Also, NICD (I) activates Fringe and, because of that, we considered that the fraction of glycosylated Notch increases constitutively with the increase of NICD (I). We point out that some time delay might be important in this process; the Fringe produced at time t should modify Notch only at a later time $t + \delta$.

For simplicity, let us first consider the effect of Fringe only in the *trans*-interaction between Notch–Delta. The *cis*-interaction between Notch–Delta, and both *cis*- and *trans*-interaction between Notch and Jagged are omitted; however, the same argument can be used to understand the changes in these interactions due to glycosylation.

Let us consider the following reaction: Notch of the cell N binds to external Delta D_{ext} creating a complex ND_{ext},

$$[N] + [D_{ext}] \rightleftharpoons [ND_{ext}]. \quad \textbf{[S1]}$$

The equations for this reaction for both the glycosylated Notch and the nonglycosylated Notch, N^* and N', respectively, are given by

$$\frac{dN^*}{dt} = N_0^* H^S(I, \lambda_N) - \gamma N^* - \left(k_{T+}^* N^* D_{ext} - k_{T-}^* \left[N^* D_{ext}\right]\right), \quad \textbf{[S2]}$$

$$\frac{dN'}{dt} = N_0' H^S(I, \lambda_N) - \gamma N' - \left(k_{T+}' N' D_{ext} - k_{T-}' \left[N' D_{ext}\right]\right), \quad \textbf{[S3]}$$

where the k_{T+} and k_{T-} represent the binding and unbinding rate, respectively. Then, the equations that represent the $[ND_{ext}]$ complex are

$$\frac{d\left[N^* D_{ext}\right]}{dt} = k_{T+}^* N^* D_{ext} - k_{T-}^* \left[N^* D_{ext}\right] - k_I^* \left[N^* D_{ext}\right], \quad \textbf{[S4]}$$

$$\frac{d\left[N' D_{ext}\right]}{dt} = k_{T+}' N' D_{ext} - k_{T-}' \left[N' D_{ext}\right] - k_I' \left[N' D_{ext}\right], \quad \textbf{[S5]}$$

where the last term represents the release of the signal (NICD) that occurs with a rate k_I and leads to the degradation of both proteins. Assuming the quasi-steady state for $[N^* D_{ext}]$ and $[N' D_{ext}]$, we obtain

$$\left[N^* D_{ext}\right] = \frac{k_{T+}^*}{k_{T-}^* + k_I^*} N^* D_{ext}, \quad \textbf{[S6]}$$

$$\left[N' D_{ext}\right] = \frac{k_{T+}'}{k_{T-}' + k_I'} N' D_{ext}. \quad \textbf{[S7]}$$

Now, let us define $N = N' + N^*$. We can write $N' = (1-f)N$ and $N^* = fN$, where $f : [0, 1]$ represents the fraction of Notch that has been modified by Fringe.

Then,

$$\frac{dN}{dt} = N_0 H^S(I, \lambda_N) - \gamma N - k_T(1 + af)D_{ext}, \quad \textbf{[S8]}$$

where

$$k_T = \frac{k'_{T+}k'_I}{k'_{T-} + k'_I} \quad \textbf{[S9]}$$

and

$$a = \frac{k^*_{T+}k^*_I}{k'_{T+}k'_I} \frac{(k'_{T-} + k'_I)}{\left(k^*_{T-} + k^*_I\right)} - 1. \quad \textbf{[S10]}$$

Similar procedure can be done for both Notch–Jagged and *cis*-interaction. Then, the model becomes

$$\frac{dN}{dt} = N_0 H^S(I, \lambda_N) - N\left[(k_C D + k_T D_{ext})[1 + a_d f(I)] + (k_C J + k_T J_{ext})\left[1 + a_j f(I)\right]\right] - \gamma_N N, \quad \textbf{[S11]}$$

$$\frac{dD}{dt} = D_0 H^S(I, \lambda_D) - k_C DN[1 + a_d f(I)] - k_T DN_t - \gamma_D D, \quad \textbf{[S12]}$$

$$\frac{dJ}{dt} = J_0 H^S(I, \lambda_J) - k_C JN\left[1 + a_j f(I)\right] - k_T JN_t - \gamma_J J, \quad \textbf{[S13]}$$

$$\frac{dI}{dt} = k_T N\left(D_{ext}[1 + a_d f(I)] + J_{ext}\left[1 + a_j f(I)\right]\right) - \gamma_I I. \quad \textbf{[S14]}$$

We considered that $f = H^+(I)$ is a positive Hill function that increases when the signal increases. In this case, we can rewrite the term related to the Fringe effect in terms of shifted Hill functions: $k(I) = k[1 + aH^+(I)] = kH^S(I, \lambda^F)$ where $\lambda^F = 1 + a$. Then, the equations above become

$$\frac{dN}{dt} = N_0 H^S(I, \lambda_N) - N\left[(k_C D + k_T D_{ext})H^S\left(I, \lambda^F_D\right) + (k_C J + k_T J_{ext})H^S\left(I, \lambda^F_J\right)\right] - \gamma_N N, \quad \textbf{[S15]}$$

$$\frac{dD}{dt} = D_0 H^S(I, \lambda_D) - k_C H^S\left(I, \lambda^F_D\right)ND - k_T DN_t - \gamma_D D, \quad \textbf{[S16]}$$

$$\frac{dJ}{dt} = J_0 H^S(I, \lambda_J) - k_C H^S\left(I, \lambda^F_J\right)NJ - k_T JN_t - \gamma_J J, \quad \textbf{[S17]}$$

$$\frac{dI}{dt} = k_T N\left[D_{ext} H^S\left(I, \lambda^F_D\right) + J_{ext} H^S\left(I, \lambda^F_J\right)\right] - \gamma_I I. \quad \textbf{[S18]}$$

S3. Two-Cell Model Equations

In the next subsections we describe the model for two interaction cells for the three models: Notch–Delta only (*N*–D), Notch–Delta–Jagged (*N*–D–J), and the model considering the Fringe effect (*N*–D–J–F). The model represents the dynamic of the proteins for the cell 1 that interacts with cell 2. Similar equations represent the dynamic of the proteins in cell 2.

N–D Model.

$$\frac{dN_1}{dt} = N_0 H^S(I_1, \lambda_N) - N_1(k_C D_1 + k_T D_2) - \gamma N_1, \quad \textbf{[S19]}$$

$$\frac{dD_1}{dt} = D_0 H^S(I_1, \lambda_D) - D_1(k_C N_1 + k_T N_2) - \gamma D_1, \quad \textbf{[S20]}$$

$$\frac{dI_1}{dt} = k_T N_1 D_2 - \gamma_I I_1. \quad \textbf{[S21]}$$

N–D–J Model.

$$\frac{dN_1}{dt} = N_0 H^S(I_1, \lambda_N) - N_1[k_C(D_1 + J_1) + k_T(D_2 + J_2)] - \gamma N_1, \quad \textbf{[S22]}$$

$$\frac{dD_1}{dt} = D_0 H^S(I_1, \lambda_D) - D_1(k_C N_1 + k_T N_2) - \gamma D_1, \quad \textbf{[S23]}$$

$$\frac{dJ_1}{dt} = J_0 H^S(I_1, \lambda_J) - J_1(k_C N_1 + k_T N_2) - \gamma J_1, \quad \textbf{[S24]}$$

$$\frac{dI_1}{dt} = k_T N_1(D_2 + J_2) - \gamma_I I_1. \quad \textbf{[S25]}$$

N–D–J–F Model.

$$\frac{dN_1}{dt} = N_0 H^S(I_1, \lambda_N) - N_1\left[(k_C D_1 + k_T D_2)H^S\left(I_1, \lambda^F_D\right) + (k_C J_1 + k_T J_2)H^S\left(I_1, \lambda^F_J\right)\right] - \gamma N_1, \quad \textbf{[S26]}$$

$$\frac{dD_1}{dt} = D_0 H^S(I_1, \lambda_D) - k_C H^S\left(I_1, \lambda^F_D\right)N_1 D_1 - k_T H^S\left(I_2, \lambda^F_D\right)D_1 N_2 - \gamma D_1, \quad \textbf{[S27]}$$

$$\frac{dJ_1}{dt} = J_0 H^S(I_1, \lambda_J) - k_C H^S\left(I_1, \lambda^F_J\right)N_1 J_1 - k_T H^S\left(I_2, \lambda^F_J\right)J_1 N_2 - \gamma J_1, \quad \textbf{[S28]}$$

$$\frac{dI_1}{dt} = k_T N_1\left[D_2 H^S\left(I_1, \lambda^F_D\right) + J_2 H^S\left(I_1, \lambda^F_J\right)\right] - \gamma_I I_1. \quad \textbf{[S29]}$$

S4. Dimensionless Version of the Model

To write the dimensionless version of the model, let us define the dimensionless variables: $n = \gamma N/N_0$, $d = \gamma D/D_0$, $j = \gamma J/J_0$, and $i = I/I_0$. Note that N_0, D_0, and J_0 represent the production rate of the proteins (in molec/h), whereas I_0 is the threshold of the Hill function (in molec).

For the case of Notch–Delta model, Eqs. **5**–**7** become

$$\tau\frac{dn}{dt} = \left(1 + \frac{i^p}{1 + i^p}\right) - \alpha_d nd - (\beta_d + 1)n, \quad \textbf{[S30]}$$

$$\tau\frac{dd}{dt} = \frac{1}{1 + i^p} - \alpha_n nd - (\beta_n + 1)d, \quad \textbf{[S31]}$$

$$\frac{di}{dt} = \beta_i\beta_d\, n - i, \quad \textbf{[S32]}$$

where $t \equiv \mathrm{t}\gamma_I$, $\tau \equiv \gamma_I/\gamma$, $\alpha_d \equiv k_c D_0/\gamma^2$, $\beta_d \equiv k_t D_{ext}/\gamma$, $\alpha_n \equiv k_c N_0/\gamma^2$, $\beta_n \equiv k_t N_{ext}/\gamma$, and $\beta_i \equiv (N_0)/(I_0\gamma_I)$.

Similarly, for the case of Notch–Delta–Jagged model, Eqs. **1**–**4** become

$$\tau\frac{dn}{dt}=\left(1+\frac{i^p}{1+i^p}\right)-n\left(\alpha_d d+\alpha_j j\right)-(\beta+1)n, \quad \textbf{[S33]}$$

$$\tau\frac{dd}{dt}=\frac{1}{1+i^p}-\alpha_n n d-(\beta_n+1)d, \quad \textbf{[S34]}$$

$$\tau\frac{dj}{dt}=\left(1+\frac{i^{p_j}}{1+i^{p_j}}\right)-\alpha_n n j-(\beta_n+1)j, \quad \textbf{[S35]}$$

$$\frac{di}{dt}=\beta_i\beta n-i, \quad \textbf{[S36]}$$

where $\alpha_j=k_c J_0/\gamma^2$, $\beta=\beta_d+\beta_j$, and $\beta_j=k_r J_{ext}/\gamma$.

Lastly, the dimensionless version of the Notch–Delta–Jagged–Fringe model (Eqs. **8**–**11**) is

$$\begin{aligned}\tau\frac{dn}{dt}=&\left(1+\frac{i^p}{1+i^p}\right)-n\left[\alpha_d d H^S\left(i,\lambda_D^F\right)+\alpha_j j H^S\left(i,\lambda_J^F\right)\right]\\&-n\left[\beta_d H^S\left(i,\lambda_D^F\right)+\beta_j H^S\left(i,\lambda_J^F\right)+1\right],\end{aligned} \quad \textbf{[S37]}$$

$$\tau\frac{dd}{dt}=\frac{1}{1+i^p}-\alpha_n n d H^S\left(i,\lambda_D^F\right)-(\beta_n+1)d, \quad \textbf{[S38]}$$

$$\tau\frac{dj}{dt}=\left(1+\frac{i^{p_j}}{1+i^{p_j}}\right)-\alpha_n n j H^S\left(i,\lambda_J^F\right)-(\beta_n+1)j, \quad \textbf{[S39]}$$

$$\frac{di}{dt}=\beta_i n\left[\beta_d H^S\left(i,\lambda_D^F\right)+\beta_j H^S\left(i,\lambda_J^F\right)\right]-i. \quad \textbf{[S40]}$$

S5. Parameter Sensitivity Analysis

We first perform the sensitivity of the model applied to the steady state by quantifying the changes of the signal as function of the changes of the parameters. Each parameter was increased and decreased its value 10% off its values described in Table S1. The relative change in the steady state of the signal is presented in Fig. S1. These results indicate that the most important parameters—in which a change in its value by 10% generates a higher change in the signal—are the same in the three models, thus showing a good consistency among the models. The most important parameters are the production and degradation rate of Notch N_0 and γ_N, respectively, the production rate of Delta D_0, and the transactivation rate k_T. Note that in this analysis we considered different parameters for the degradation rate of Notch, Delta, and Jagged $(\gamma_N,\gamma_D,\gamma_J)$ whereas in the model we considered them to be the same (γ). To evaluate the influence of these four parameters in the shape of the bifurcations curves, we changed by 10% the values of each parameter. The limit point where the system changes from one state to the other is very sensitive to changes in these parameters (Fig. S2); however, the overall behavior of the circuit remains the same, therefore suggesting a good robustness of the model.

We also evaluate the relative changes in the steady state of the signal (NICD) with respect to changes in the parameters for the dimensionless version of the model. This analysis shows that the most sensitive parameters are the ones related to the quadratic term of the equations: $\alpha_N,\alpha_D,\alpha_J$, and the ones related to the term of the production of the signal: β_I,β_D,β_J. All these parameters are related to the N_0, γ_N, D_0, and k_T, therefore showing that both sensitivity analyses are consistent with each other.

For most parameters, changes in value of 10% lead to very small changes in the signal. On one hand, this means that the results and predictions of the model are quite robust by changes in the parameters. On the other hand, this means that some extra caution must be taken when planning an experimental validation of the values of these parameters. The most simple experiment for validating this model is to measure the intensity of the signal using a report protein. If this kind of experiment is used to fit the parameters, we should expect that many parameters will have a large range of values in which they fit the experimental data well. This should occur once changes in the majority of the parameters lead to small changes in the signal, therefore characterizing the model as sloppy (8). For this reason, experiments to validate the values of the parameters should be carefully designed.

S6. Considering the Effect of both Soluble and Membrane-Bound Ligands

Experimental evidence suggests that membrane-bound ligands should activate the signal strongly compared with soluble ligands. This happens because soluble ligand does not have enough mechanical pulling force to activate the signal (9). However, alternative mechanisms such as ligand multimerization can lead to sufficient mechanical force for ligand activation (10). Further evidence that membrane-bound should activate the signal strongly is that lower lateral mobility of the ligand leads to higher signaling (11). Therefore, a model that considers both soluble and membrane-bound ligands should have two terms in Notch equation for interaction with both forms of these ligands. For example, the model presented in Eqs. **1**–**4** would be

$$\begin{aligned}\frac{dN}{dt}=&N_0 H^{S+}(I)-k_C N(D+J)-k_T^m N\left(D_{ext}^m+J_{ext}^m\right)\\&-k_T^s N\left(D_{ext}^s+J_{ext}^s\right)-\gamma N,\end{aligned} \quad \textbf{[S41]}$$

$$\frac{dD}{dt}=D_0 H^{S-}(I)-k_C D N-k_T^m D N_{ext}-\gamma D, \quad \textbf{[S42]}$$

$$\frac{dJ}{dt}=J_0 H^{S+}(I)-k_C J N-k_T^m J N_{ext}-\gamma J, \quad \textbf{[S43]}$$

$$\frac{dI}{dt}=N\left[k_T^m\left(D_{ext}^m+J_{ext}^m\right)+k_T^s\left(D_{ext}^s+J_{ext}^s\right)\right]-\gamma_I I, \quad \textbf{[S44]}$$

where D_{ext}^m and J_{ext}^m represent membrane-bound Delta and Jagged, respectively, and D_{ext}^s and J_{ext}^s represent soluble Delta and Jagged, respectively. k_T^m and k_T^s represent the transactivation rate for membrane-bound ligands and for soluble ligands, respectively, and it is expected that $k_T^m>k_T^s$.

S7. Temporal Dynamics and Stochastic Simulations

To evaluate the amount of time for reaching the steady state, we represented the dynamics of 100 cells starting from different initial conditions. For most cases, one of the three possible equilibrium states was reached up to 100 h. This time scale is consistent with the characteristic developmental time scale, Fig. S3*A*. Similar results are found for a stochastic dynamics using the Gillespie algorithm, Fig. S3*B*. Interestingly the intermediate S/R state presents a large basin of attraction, Fig. S3*C*.

1. Sprinzak D, et al. (2010) Cis-interactions between Notch and Delta generate mutually exclusive signalling states. *Nature* 465(7294):86–90.

2. Brabletz S, et al. (2011) The ZEB1/miR-200 feedback loop controls Notch signalling in cancer cells. *EMBO J* 30(4):770–782.

3. Gill JG, et al. (2011) Snail and the microRNA-200 family act in opposition to regulate epithelial-to-mesenchymal transition and germ layer fate restriction in differentiating ESCs. *Stem Cells* 29(5):764–776.
4. Timmerman LA, et al. (2004) Notch promotes epithelial-mesenchymal transition during cardiac development and oncogenic transformation. *Genes Dev* 18(1):99–115.
5. Wang MM (2011) Notch signaling and Notch signaling modifiers. *Int J Biochem Cell Biol* 43(11):1550–1562.
6. Amsen D, et al. (2004) Instruction of distinct CD4 T helper cell fates by different notch ligands on antigen-presenting cells. *Cell* 117(4):515–526.
7. Hicks C, et al. (2000) Fringe differentially modulates Jagged1 and Delta1 signalling through Notch1 and Notch2. *Nat Cell Biol* 2(8):515–520.
8. Gutenkunst RN, et al. (2007) Universally sloppy parameter sensitivities in systems biology models. *PLOS Comput Biol* 3(10):1871–1878.
9. Musse AA, Meloty-Kapella L, Weinmaster G (2012) Notch ligand endocytosis: mechanistic basis of signaling activity. *Semin Cell Dev Biol* 23(4):429–436.
10. Hicks C, et al. (2002) A secreted Delta1-Fc fusion protein functions both as an activator and inhibitor of Notch1 signaling. *J Neurosci Res* 68(6):655–667.
11. Narui Y, Salaita K (2013) Membrane tethered delta activates notch and reveals a role for spatio-mechanical regulation of the signaling pathway. *Biophys J* 105(12): 2655–2665.

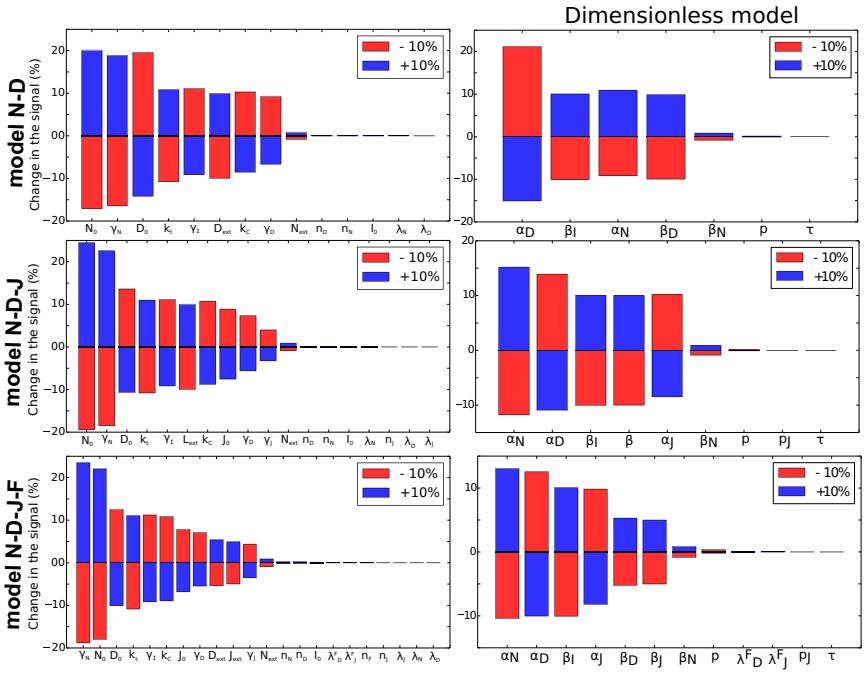

Fig. S1. Parameter sensitivity analysis. Relative changes in the steady state of the signal (NICD) with respect to their value in the stable state when each parameter is increased and decreased by 10% over its standard value described in Table S1.

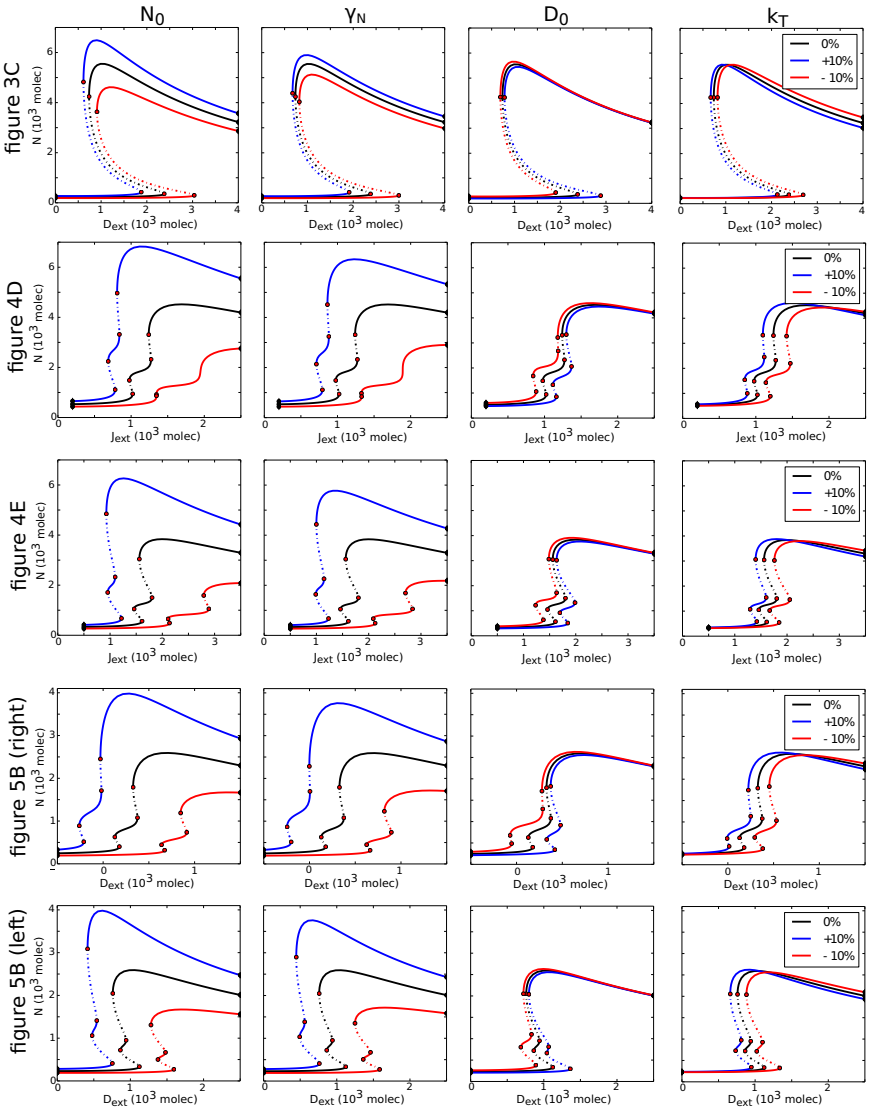

Fig. S2. Changes in the bifurcation curves with respect to changes in 10% of the values of the parameters N_0, γ_N, D_0, and k_T. Each line represents the changes in the bifurcations curves present in the main text: Figs. 3*C*, 4 *D* and *E*, 5*B* (*Right*), and 5*B* (*Left*), respectively.

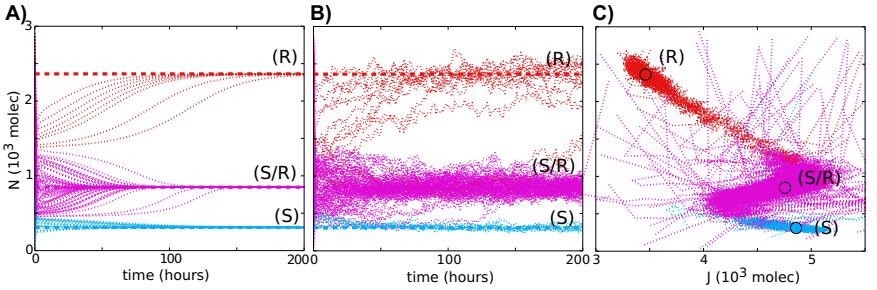

Fig. S3. (*A*) Concentration of Notch (N) as a function of time for 100 trajectories. The initial conditions were chosen randomly. It shows that irrespective of the initial conditions, all trajectories converge to one of the three steady states. (*B*) Dynamic representation of 100 trajectories simulated using Gillespie algorithm. The initial conditions were chosen randomly. Concentration of Notch (N) as a function of time. (*C*) Representation of the trajectories presented in *B* in the phase plane (*JxN*).

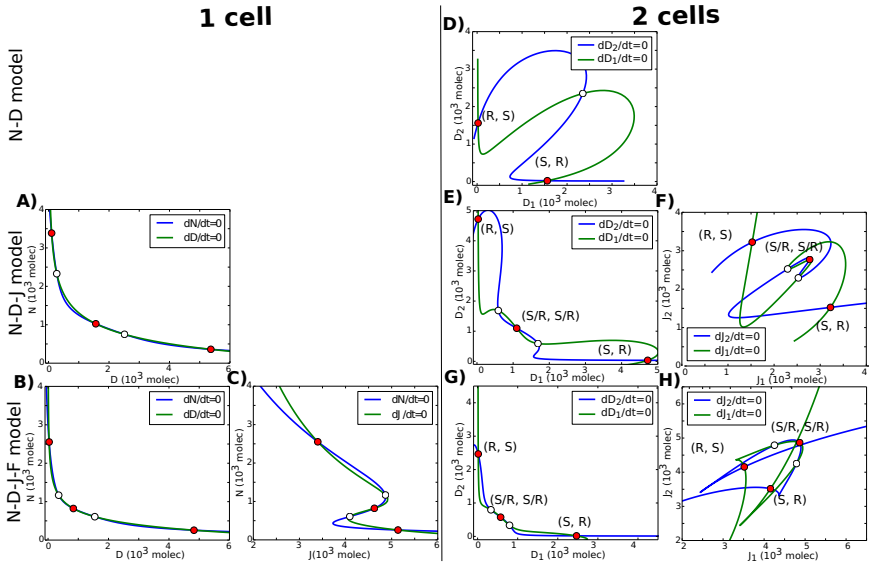

Fig. S4. (*Left*) Nullclines for the case of one cell for: (*A*) $N \times D$ for the *N*–D–J model; (*B*) $N \times D$ for the *N*–D–J–F model; (*C*) $N \times J$ for the *N*–D–J–F model. Unfilled circle represents unstable steady states, and the red filled circles represent the two stable states. (*Right*) Nullclines for the case of two interacting cells for: (*D*) $D_1 \times D_2$ for the *N*–D model; (*E*) $D_1 \times D_2$ for the *N*–D–J model; (*F*) $J_1 \times J_2$ for the *N*–D–J model; (*G*) $D_1 \times D_2$ for the *N*–D–J–F model; (*H*) $J_1 \times J_2$ for the *N*–D–J–F model.

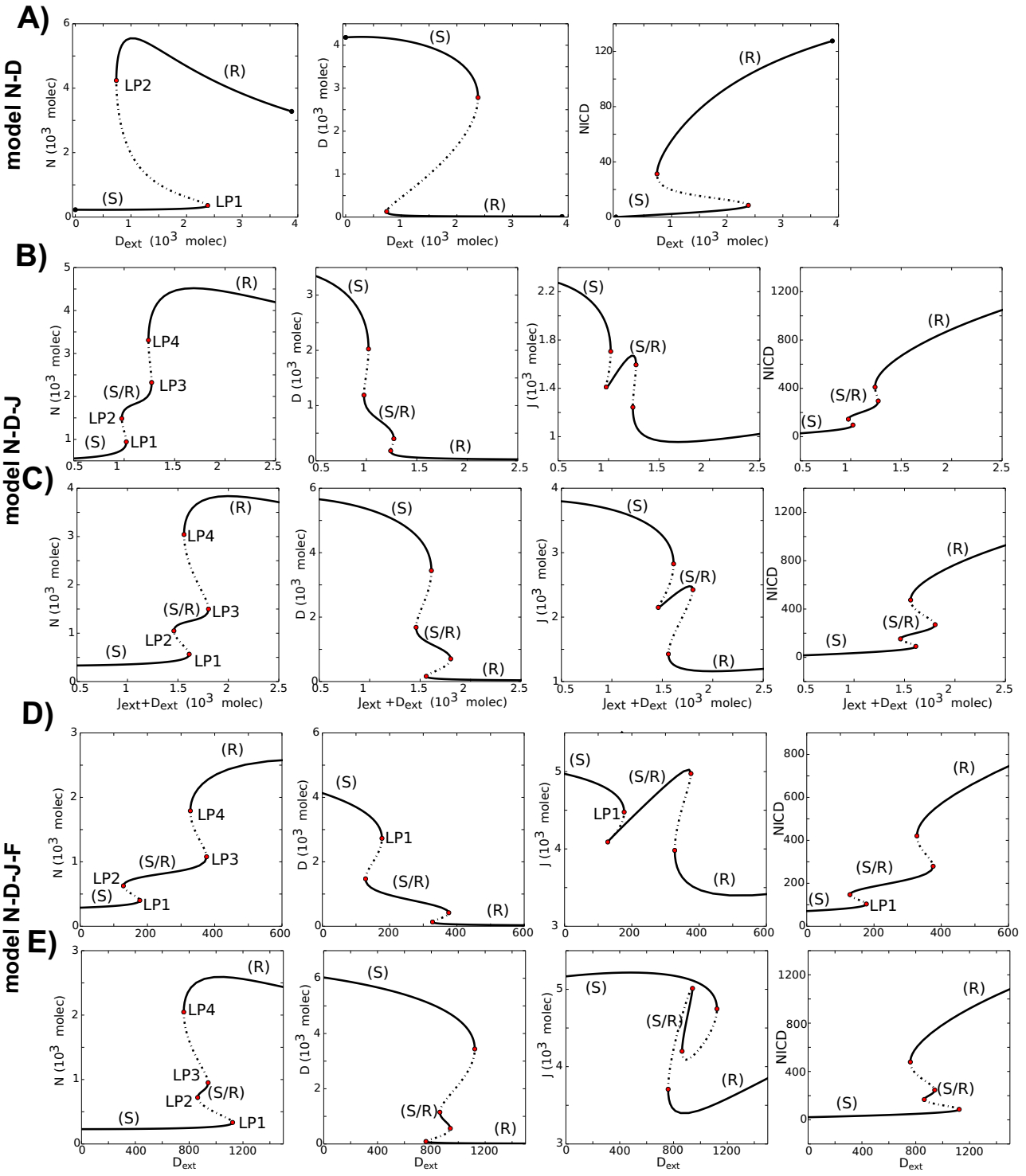

Fig. S5. Bifurcation curves for the levels of different proteins. In the main text only the curves for Notch levels are presented in Figs. 3*C*, 4 *D* and *E*, 5*B* (*Right*), and 5*B* (*Left*), respectively. Here, we also include the eigenvalues and normal form coefficient for each limit point. For all limit points, the normal form coefficient is higher than zero and therefore the system is nondegenerate. (*A*) Bifurcation for the N–D model (see Fig. 3*C* in the main text): $N_{ext} = 500$. (*B*) Bifurcation for the *N*–D–J model (Fig. 4*D*): $N_{ext} = 3{,}000$ and $Y_{ext} = D_{ext} + J_{ext}$. (*C*) Bifurcation for the *N*–D–J model (Fig. 4*E*): $N_{ext} = 1{,}000$. (*D*) bifurcation for the *N*–D–J–F model (Fig. 5*B*, *Right*): $N_{ext} = 500$, $J_{ext} = 3{,}000$. (*E*) Bifurcation for the *N*–D–J–F model (Fig. 5*B*, *Left*): $N_{ext} = 500$, $J_{ext} = 1{,}000$. Normal form coefficients and eigenvalues: (*A*) ($a_1 = 3.95e^{-5}$, $a_2 = 2.10e^{-5}$), eigenvalues ($[N,D,I]_1 = [-1.87e^{-0}, 2.82e^{-8}, -5.43e^{-1}]$, $[N,D,I]_2 = [-2.28e^{-0}, -1.15e^{-8}, -6.6e^{-1}]$). (*B*) ($a_1 = 3.82e^{-5}$, $a_2 = 6.24e^{-5}$, $a_3 = 3.39e^{-5}$, $a_4 = 1.75e^{-5}$), eigenvalues ($[N,D,J,I]_1 = [-2.58e^{-0}, 1.24e^{-7}, -7.21e^{-1}, -6.51e^{-1}]$, $[N,D,J,I]_2 = [-2.31e^{-0}, 1.32e^{-7}, -9.92e^{-1}, -6.26e^{-1}]$, $[N,D,J,I]_3 = [-2.40e^{-0}, 1.54e^{-8}, -6.75e^{-1}, -1.41e^{-0}]$, $[N,D,J,I]_4 = [-2.58e^{-0}, -1.90e^{-0}, -1.99e^{-8}, -6.97e^{-1}]$). (*C*) ($a_1 = 2.33e^{-5}$, $a_2 = 6.10e^{-5}$, $a_3 = 6.27e^{-5}$, $a_4 = 2.75e^{-5}$), eigenvalues ($[N,D,J,I]_1 = [-3.70e^{-0}, 9.97e^{-8}, -5.45e^{-1}, -4.33e^{-1}]$, $[N,D,J,I]_2 = [-2.74e^{-0}, -7.23e^{-8}, -6.74e^{-1}, -5.22e^{-1}]$, $[N,D,J,I]_3 = [-2.58e^{-0}, 9.59e^{-8}, -9.01e^{-1}, -5.78e^{-1}]$, $[N,D,J,I]_4 = [-2.47e^{-0}, -1.67e^{-0}, 1.43e^{-8}, -6.78e^{-1}]$). (*D*) ($a_1 = 1.68e^{-5}$, $a_2 = 4.11e^{-5}$, $a_3 = 5.43e^{-5}$, $a_4 = 2.10e^{-5}$), eigenvalues ($[N,D,J,I]_1 = [-4.58e^{-0}, -6.86e^{-1}, -2.73e^{-8}, -2.82e^{-1}]$, $[N,D,J,I]_2 = [-3.54e^{-0}, -8.53e^{-1}, -6.45e^{-8}, -2.73e^{-1}]$, $[N,D,J,I]_3 = [-2.81e^{-0}, -1.32e^{-0}, 1.04e^{-7}, -3.24e^{-1}]$, $[N,D,J,I]_4 = [-2.49e^{-0}, -1.85e^{-0}, -9.24e^{-8},$

Legend continued on following page

$-4.75e^{-1}$]). (*E*) ($a_1 = 2.55e^{-5}$), $a_2 = 9.33e^{-5}$, $a_3 = 1.23e^{-4}$, $a_4 = 3.80e^{-5}$, eigenvalues ($[N,D,J,I]_1 = [-5.13e^{-0}, -5.55e^{-1}, -2.25e^{-8}, -2.58e^{-1}]$, $[N,D,J,I]_2 = [-3.31e^{-0}, -8.80e^{-1}, 4.62e^{-8}, -1.85e^{-1}]$, $[N,D,J,I]_3 = [-2.98e^{-0}, -1.15e^{-0}, -5.41e^{-8}, -2.11e^{-1}]$, $[N,D,J,I]_4 = [-2.73e^{-0}, -1.80e^{-0}, 6.95e^{-8}, -4.34e^{-1}]$).

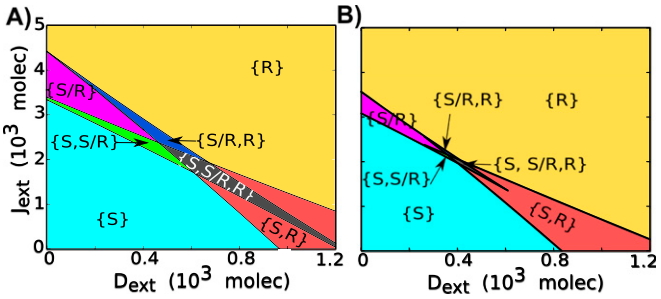

Fig. S6. Phase diagram. (*A*) Same as Fig. 5*B* (*Center*). (*B*) Same as *A* for $n_j = 4$. For values of $n_j < 4$ the circuit does not present tristability, given all other parameters chosen as given in Table S1.

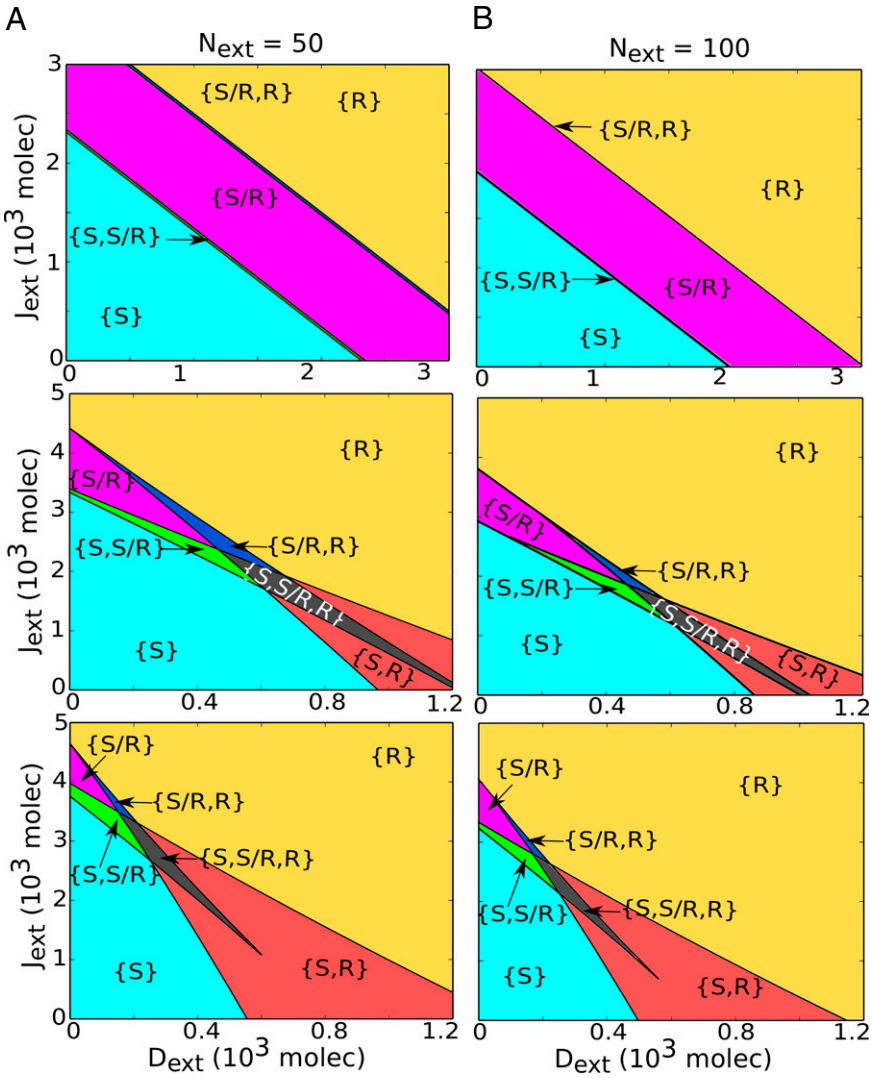

Fig. S7. Phase diagram. (*A*) Same as Fig. 5 (*Center*). (*B*) Same as *A* for $N_{ext} = 1{,}000$.

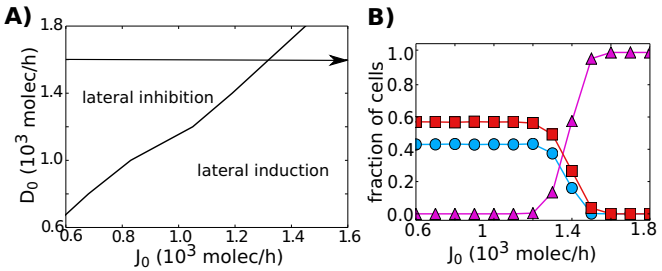

Fig. S8. (*A*) Phase diagram as a function of the production rate of Jagged (J_0) and production rate of Delta (D_0). As the production of Jagged (J_0) increases, the cells tend to keep the same fate (lateral induction). Conversely, as the production of Delta (D_0) increases, the cells tend to adopt alternate fate. (*B*) Same as Fig. 7*D* ($D_0 = 1{,}600$ molec/h).

Table S1. Parameter values used in the simulations

Parameter	Value	Unit
γ	0.1	time^{-1}(h^{-1})
γ_I	0.5	time^{-1}(h^{-1})
N_0	500*, 1,600†, 1,400‡	Number of proteins
D_0	1,000*, 1,800†, 1,600‡	Number of proteins
J_0	1,200†,‡	Number of proteins
k_T	5e^{-5}	time^{-1}(h^{-1})
k_C	5e^{-4}	time^{-1}(h^{-1})
I_0	200	Number of proteins
n_N,n_D	2.0	Dimensionless
n_J	5.0	Dimensionless
n_F	1.0	Dimensionless
λ_N,λ_J	2.0	Dimensionless
λ_D	0.0	Dimensionless
λ_D^F	3.0	Dimensionless
λ_J^F	0.3	Dimensionless

*Values for Fig. 3.
†Values for Fig. 4.
‡Values for Fig. 5. Values for Figs. 6 and 7 are the same as for Fig. 5.